

The Signal Transducer NPH3 Integrates the Phototropin1 Photosensor with PIN2-Based Polar Auxin Transport in *Arabidopsis* Root Phototropism

Yinglang Wan,^a Jan Jasik,^{b,c,1} Li Wang,^a Huaiqing Hao,^a Dieter Volkmann,^b Diedrik Menzel,^b Stefano Mancuso,^d František Baluška,^{b,e,1} and Jinxing Lin^{a,1,2}

^aKey Laboratory of Plant Molecular Physiology, Institute of Botany, Chinese Academy of Sciences, Beijing 100093, China

^bInstitute of Cellular and Molecular Botany, University of Bonn, D-53115 Bonn, Germany

^cDepartment of Molecular Genetics, Leibniz Institute of Plant Genetics and Crop Plant Research, D-06466 Gatersleben, Germany

^dDepartment of Plant, Soil, and Environmental Science, University of Florence, 50019 Sesto Fiorentino, Italy

^eInstitute of Botany, Slovak Academy of Sciences, SK-845 23 Bratislava, Slovak Republic

Under blue light (BL) illumination, *Arabidopsis thaliana* roots grow away from the light source, showing a negative phototropic response. However, the mechanism of root phototropism is still unclear. Using a noninvasive microelectrode system, we showed that the BL sensor phototropin1 (*phot1*), the signal transducer NONPHOTOTROPIC HYPOCOTYL3 (NPH3), and the auxin efflux transporter PIN2 were essential for BL-induced auxin flux in the root apex transition zone. We also found that PIN2-green fluorescent protein (GFP) localized to vacuole-like compartments (VLCs) in dark-grown root epidermal and cortical cells, and *phot1*/NPH3 mediated a BL-initiated pathway that caused PIN2 redistribution to the plasma membrane. When dark-grown roots were exposed to brefeldin A (BFA), PIN2-GFP remained in VLCs in darkness, and BL caused PIN2-GFP disappearance from VLCs and induced PIN2-GFP-FM4-64 colocalization within enlarged compartments. In the *nph3* mutant, both dark and BL BFA treatments caused the disappearance of PIN2-GFP from VLCs. However, in the *phot1* mutant, PIN2-GFP remained within VLCs under both dark and BL BFA treatments, suggesting that *phot1* and NPH3 play different roles in PIN2 localization. In conclusion, BL-induced root phototropism is based on the *phot1*/NPH3 signaling pathway, which stimulates the shootward auxin flux by modifying the subcellular targeting of PIN2 in the root apex transition zone.

INTRODUCTION

Plant roots serve to fix the plant body in the soil and provide plants with water and nutrients. Roots need to sense and respond appropriately to a diversity of environmental signals, such as gravity, mechanical impedance, light, humidity, oxygen, and essential nutrients, as well as allelochemicals exuded from neighboring roots, to develop their optimal form or adapt to their environment conditions (Monshausen and Gilroy, 2009). Although phototropic responses in roots were discovered and analyzed some time ago, knowledge of root phototropism is surprisingly poor when compared with that of root gravitropism (Boonsirichai et al., 2002; Correll and Kiss, 2002; Whippon and Hangarter, 2006; Holland et al., 2009; Takahashi et al., 2009).

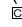
The classic Cholodny-Went theory postulates that both gravitropism and phototropism are determined by the asymmetric

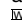
distribution of the phytohormone auxin. The current discovery and analysis of auxin efflux transporters, the PIN-formed proteins (PINs), supports this hypothesis by describing a sensitive, adjustable network of five PINs (PIN 1, 2, 3, 4, and 7) that drive polar auxin transport in the root apex (Bliilou et al., 2005; Kleine-Vehn and Friml, 2008; Baluška et al., 2010). However, polar PIN localization is not static but undergoes constant recycling between the plasma membrane (PM) and endosomal compartments (Robert and Friml, 2009). Recent studies indicate that blue light (BL) determines the localization and distribution of PIN1 and PIN3 in hypocotyl cells (Blakeslee et al., 2004; Ding et al., 2011) and PIN2 in root cells (Kleine-Vehn et al., 2008; Laxmi et al., 2008). Laxmi et al. (2008) reported that a mutation of transcription factor HY5, which is regulated by the blue and red light receptors, phytochromes and cryptochromes, respectively (Lau and Deng, 2010), decreases PM targeting of PIN2 via endosomal trafficking and that the CONSTITUTIVE PHOTOMORPHOGENIC9 complex mediates the proteasome-dependent degradation of PIN2 via its targeting into lytic vacuoles (Laxmi et al., 2008). Retromer components, such as SORTING NEXIN1 and VACUOLAR PROTEIN SORTING29, play a key role in resorting PIN2 into vacuoles under dark conditions and also in retrieving PIN2 from vacuoles back to the PM-targeted recycling pathway under light illumination (Kleine-Vehn et al., 2008). However, whether the phototropin photoreceptors (*phot*s) are relevant to PIN2 cellular fate or whether

¹ These authors contributed equally to this work.

² Address correspondence to linjx@ibcas.ac.cn.

The author responsible for distribution of materials integral to the findings presented in this article in accordance with the policy described in the Instructions for Authors (www.plantcell.org) is: Jinxing Lin (linjx@ibcas.ac.cn).

 Some figures in this article are displayed in color online but in black and white in the print edition.

 Online version contains Web-only data.

www.plantcell.org/cgi/doi/10.1105/tpc.111.094284

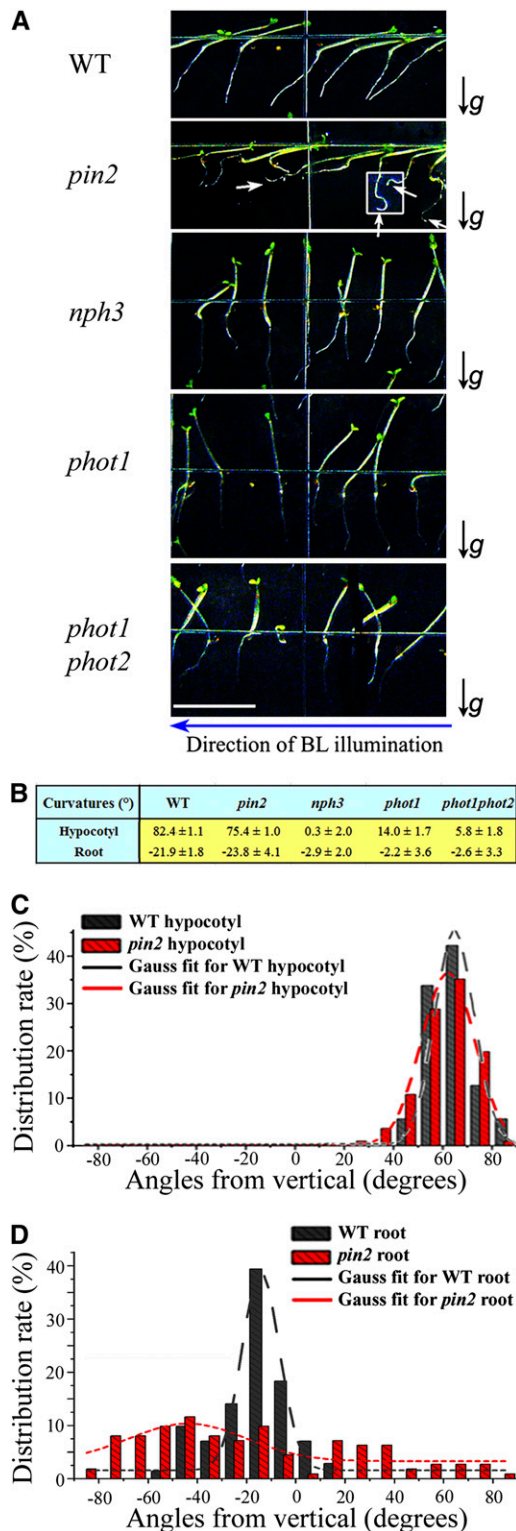


Figure 1. Analysis of Root and Hypocotyl Phototropic Curvature in *pin2*, *nph3*, *phot1*, and *phot1 phot2* Mutant Lines.

(A) Pictures were taken from 4-d-old seedlings of wild-type (WT), *pin2*, *nph3*, *phot1*, and *phot1 phot2* *Arabidopsis* grown on same vertical plates

PIN2 subcellular relocation or degradation (or both) is involved in BL-induced root phototropism is unclear. In our previous study, we reported that the BL receptor *phot1* is polarly localized on the PM of root cortical cells, showing a localization very similar to that of PIN2 (Rahman et al., 2010), and that the extent of BL-induced *phot1* internalization reflects the intensity of BL administered (Wan et al., 2008). Based on these results, we postulated a relationship between BL-induced relocation of *phot1* and endosomal recycling of PIN2 protein.

The *phots* and the PINOID protein (PID) are close homologs belonging to the same AGC kinase family (Galván-Ampudia and Offringa, 2007). PID, a Ser/Thr kinase, and a PP2A protein phosphatase regulate the root gravitropic responses by controlling the phosphorylation and dephosphorylation status (Christensen et al., 2000; Friml et al., 2004; Michniewicz et al., 2007), as well as the polar localization of PIN2 (Sukumar et al., 2009; Rahman et al., 2010). Also, a protein named MACCHI-BOU4/ENHANCER OF PINOID/NAKED PINS IN YUC MUTANTS1 (MAB4/ENP/NPY1) is closely homologous to NONPHOTOTROPIC HYPOCOTYL3 (NPH3), an essential scaffold protein, in transducing the *phot1*-initiated phototropic responses (Cheng et al., 2007; Furutani et al., 2007). Cheng et al. (2007) hypothesized that *PID/NPY1* and *phot1/NPH3* act via similar pathways to modify polar auxin transport and subsequently to regulate plant development. This hypothesis was further supported by recent reports that *NPY* genes are essential for *Arabidopsis thaliana* root gravitropic responses (Li et al., 2011) and that the MAB4/ENP/NPY1 protein also regulates the polar localization and endocytosis of PINs (Furutani et al., 2011). These reports encouraged us to investigate the roles of *phot1/NPH3* in PIN2 localization, recycling, and function.

In this study, we address the possible link between photoreception and the phototropic reaction in root tips. We measured BL-induced auxin flux in the root apices of the wild type and *pin2*, *nph3*, *phot1*, and *phot1 phot2* mutant lines and observed the cellular fate of PIN2-green fluorescent protein (GFP) under BL illumination in these lines. From the results, we postulate a BL signaling pathway involving *phot1*, NPH3, and PIN2 proteins that alters polar auxin transport and controls root negative phototropism.

under lateral BL illumination ($2 \mu\text{mol}\cdot\text{m}^{-2}\cdot\text{s}^{-1}$). White arrows indicate that the roots of *pin2* mutants showing a zigzag pattern, and two of these roots are highlighted. Bar = 5 mm.

(B) Because the root tips of *pin2* show an irregular bending pattern, we measured the separation angle from vertical in hypocotyls and roots. Data represent the mean \pm SE from three independent experiments with 20 seedlings in each line at each time.

(C) and **(D)** The relative distribution rate of the separation angle from the vertical in hypocotyls **(C)** and roots **(D)** over each 10° interval was calculated and is shown diagrammatically in columns for the wild type (gray) and *pin2* (red). The dashed curves show fitted Gaussian curves from the relative distribution of curvature values. Adjusted coefficients of determination (adjusted R^2) are recorded as wild-type hypocotyls = 0.989, *pin2* hypocotyls = 0.989, wild-type root = 0.906, and *pin2* root = 0.511.

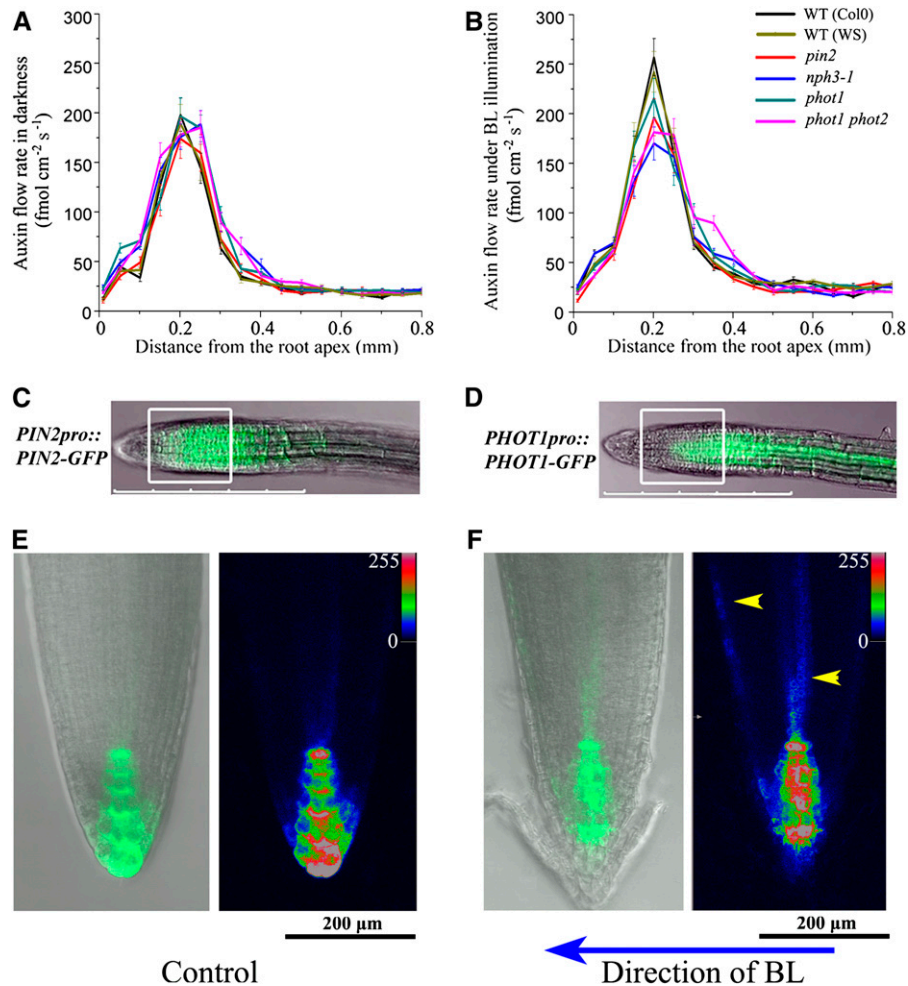


Figure 2. Auxin Flux Profiles in the Root Apex Region.

(A) and **(B)** The auxin flux profiles in the intact root apex (0 to 0.8 mm) of 4-d-old dark-grown *Arabidopsis* seedlings were measured with an auxin-specific self-referencing microelectrode in darkness **(A)** and under BL illumination **(B)**. The positive flux values represent a net auxin influx. Data are means \pm SE ($n = 12$). Mean values are listed in Supplemental Table 1 online. WT, wild type.

(C) and **(D)** The expression pattern of *PIN2_{pro}::PIN2-GFP* **(C)** and *PHOT1_{pro}::PHOT1-GFP* **(D)** and in root tips of 4-d-old dark-grown *Arabidopsis* seedlings, in which the 100- to 300-μm region is highlighted by white squares. Bars = 500 μm.

(E) Images from the GFP channel and differential interference contrast channel were combined to show the expression pattern of *DR5_{pro}::GFP* in root tips of dark-grown *Arabidopsis* seedlings (left). A pseudocolor image visualizes the signal intensities of the GFP signal (right). Color code bar indicates the relative intensities. Bar = 200 μm.

(F) The expression pattern of *DR5_{pro}::GFP* in root tips of dark-grown *Arabidopsis* seedlings after 1 h of 2 μmol·m⁻²·s⁻¹ unilateral BL illumination. Yellow arrowheads indicate increased expression of GFP in the epidermal and vascular cells. Eighty percent ($n = 10$) of the seedlings showed an asymmetric expression pattern of GFP signals after BL illumination. Color code bar indicates relative intensities. Bar = 200 μm.

RESULTS

PIN2 Is Essential for Robust Root Phototropism

The phototropic responses of the wild type (ecotype Columbia [Col]) and a null mutant line of *pin2*, named *eir1-4* (Luschnig et al., 1998), were examined under unilateral weak BL illumination (2 μmol·m⁻²·s⁻¹) (Figure 1A). Because *pin2* exhibited altered root gravitropism, the dark-grown *pin2* seedlings showed a random pattern of root growth direction (see Supplemental Figure 1 on-

line). Therefore, we illuminated the seedlings with asymmetric BL from the onset of germination. Hypocotyls of wild-type seedlings grew toward the source of the BL illumination, and roots grew away from the light source (Figure 1A). Hypocotyls of *pin2* seedlings grew in a similar pattern as the wild-type hypocotyls, whereas roots of *pin2* seedlings grew in different ways: Most of the roots showed a zigzag pattern with unilateral BL illumination (highlighted in Figure 1A), and some root tip curvatures showed a random bending direction, even bending toward the BL source (arrows in Figure 1A).

Table 1. Two-Way ANOVA for Peak Value Measurement of the Auxin Flux Rate in the Root Tip

Comparison Test	Mean Difference	Significant
Significance of differences between lines in dark condition		
Dark: wild type (Col-0) versus wild type (Ws)	−9.0	ns
Dark: wild type (Col-0) versus <i>pin2</i>	−24.1	*
Dark: wild type (Ws) versus <i>nph3</i>	−0.4	ns
Dark: wild type (Col-0) versus <i>phot1</i>	−1.5	ns
Dark: wild type (Col-0) versus <i>phot1 phot2</i>	−13.0	ns
Dark: <i>phot1</i> versus <i>phot1 phot2</i>	−11.5	ns
Dark: <i>phot1</i> versus <i>nph3</i>	−7.9	ns
Dark: <i>nph3</i> versus <i>phot1phot2</i>	−3.6	ns
Dark: <i>pin2</i> versus <i>nph3</i>	14.7	ns
Dark: <i>pin2</i> versus <i>phot1</i>	22.6	*
Dark: <i>pin2</i> versus <i>phot1phot2</i>	11.1	ns
Significance of differences between lines in BL illumination		
BL: wild type (Col-0) versus wild type (Ws)	−14.7	ns
BL: wild type (Col-0) versus <i>pin2</i>	−60.7	**
BL: wild type (Ws) versus <i>nph3</i>	−72.4	**
BL: wild type (Col-0) versus <i>phot1</i>	−41.4	*
BL: wild type (Col-0) versus <i>phot1 phot2</i>	−75.7	**
BL: <i>phot1</i> versus <i>phot1 phot2</i>	−34.3	*
BL: <i>phot1</i> versus <i>nph3</i>	−45.7	*
BL: <i>nph3</i> versus <i>phot1 phot2</i>	11.4	ns
BL: <i>pin2</i> versus <i>nph3</i>	−26.4	*
BL: <i>pin2</i> versus <i>phot1</i>	19.3	ns
BL: <i>pin2</i> versus <i>phot1 phot2</i>	−15.0	ns
Significance of differences between dark and BL condition		
Wild type (Col-0): dark versus BL	58.9	**
Wild type (Ws): dark versus BL	53.2	**
<i>pin2</i> : dark versus BL	22.3	*
<i>nph3-1</i> : dark versus BL	−18.8	ns
<i>phot1-5</i> : dark versus BL	19.0	ns
<i>phot1 phot2</i> : dark versus BL	−3.8	ns

Two-way ANOVAs were performed to compare significant differences between measured peak values of auxin flux rates. Light conditions and different mutant lines were the two sources of variation; both caused extremely significant differences ($P < 0.001$). The Bonferroni correction was then applied for comparisons among pairs. The results of comparisons are between the wild type and mutant lines under dark conditions, between the wild type and mutant lines under BL illumination, and between measurements in BL illumination and dark condition in each line. ns, no significance; *, $P < 0.05$; **, $P < 0.001$.

Hence, we measured the angles separating the root/hypocotyl tips from the vertical, rather than measuring apical curvature, to quantify the BL-modified root growth direction. As shown in Figure 1B, wild-type hypocotyls exhibited a typical positive phototropic response toward the BL source, with an average angle of 82.4° from the vertical. Roots of wild-type seedlings grew away from the light source, with an average angle from the vertical of 21.9° . In the *pin2* mutant, the lack of PIN2 protein apparently had only a small effect on hypocotyl phototropism, as inferred from an average angle of 75.3° . However, the *pin2* mutant showed strongly modified root phototropic responses; root growth direction showed a far wider distribution of angles from the vertical than the wild type, but the average angle -23.8° in *pin2* was similar to that in the wild type (Figure 1B). To further quantify the disturbed distribution rate of the *pin2* mutant, we analyzed the relative distribution of curvatures in the wild type and *pin2* as histograms (Figures 1C and 1D). Roots in the wild type and hypocotyls in both wild-type and *pin2* mutants showed a typical Gaussian distribution (adjusted $R^2 > 0.9$). However, the

distribution of BL-induced separation angles in *pin2* roots differed significantly from a Gaussian distribution (adjusted $R^2 = 0.511$), suggesting a more random distribution of root growth and strongly altered root phototropism in the *pin2* mutant under unilateral weak BL illumination.

BL-induced Auxin Flux in the Root Apex Transition Zone Is Dependent on PIN2, phot1, and NPH3

To determine the possible mechanism for the altered phototropic responses of the *pin2*, *nph3*, *phot1*, and *phot1phot2* mutants, we further measured auxin flux profiles in vivo in the root apical region using a noninvasive microelectrode system (Mancuso et al., 2005, 2007; McLamore et al., 2010), which indicated that all lines have a net rhizosphere auxin influx in the root tip region (Figures 2A and 2B). The peak auxin flow occurred at 0.20 to 0.25 mm from the root apex in dark-grown wild-type (Col-0 and Wassilewskija [Ws] ecotypes) and all mutant lines (Figures 2A and 2B), coinciding with the expression peaks of the PIN2 (Figure

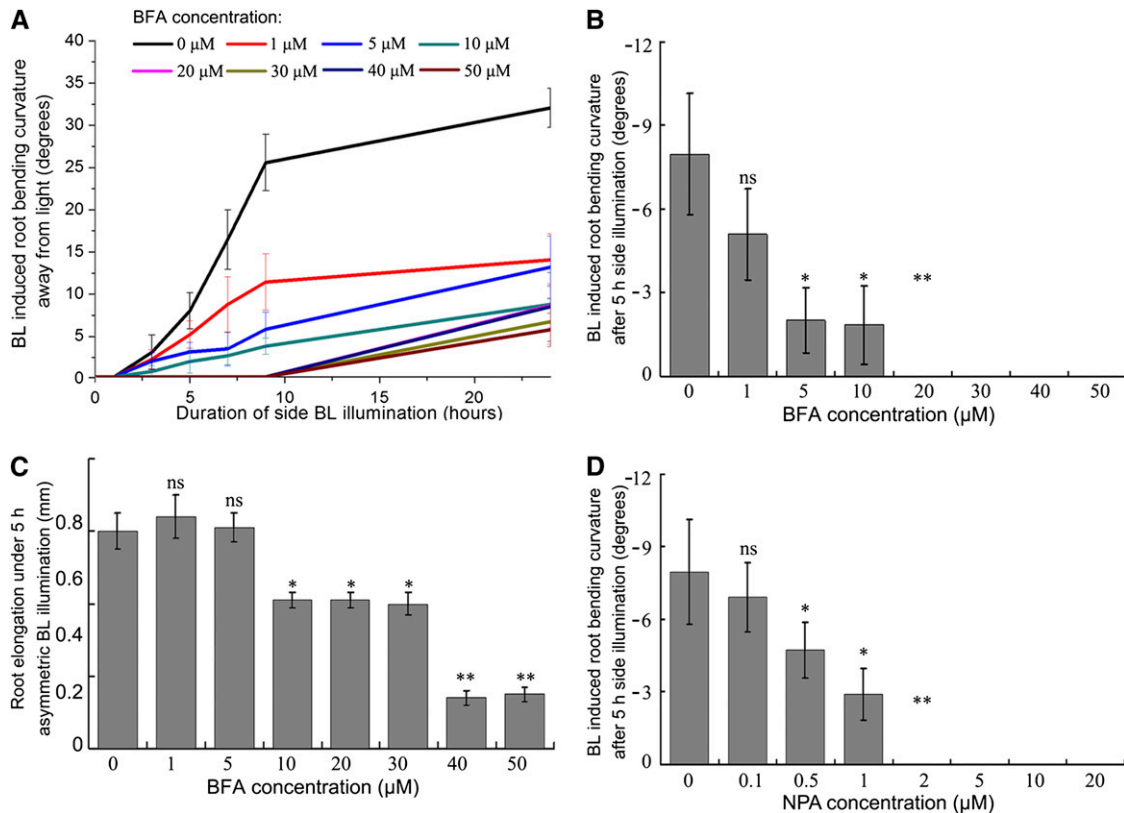


Figure 3. BFA and NPA Inhibit the BL-Induced Root Phototropism.

Three-day-old dark-grown *Arabidopsis* seedlings were transferred onto agar plates with culture medium and different concentrations of BFA and NPA and then illuminated laterally with $2 \mu\text{mol}\cdot\text{m}^{-2}\cdot\text{s}^{-1}$ BL. Images were taken every 2 h in the first 9 h from the start of illumination (see Supplemental Figure 2 online); the last measurement was taken after 24 h.

(A) Root phototropic bending curvatures were measured from the images and are shown as profiles (means \pm SE, $n = 24$).

(B) Root phototropic bending curvatures after 5 h of illumination on BFA-containing medium, presented as columns (means \pm SE, $n = 24$).

(C) Length of root elongation after 5 h of illumination on BFA-containing medium, presented as columns (means \pm SE, $n = 24$).

(D) Root phototropic bending curvatures after 5 h of illumination on NPA-containing medium, presented as columns (means \pm SE, $n = 24$).

(B) and (D) Statistical significance between chemical treatment and the control, according to Student's *t* test (ns, no significance; * $P < 0.05$; ** $P < 0.001$).

2C) and phot1 (Figure 2D) proteins. The *pin2* and *phot1* mutant lines have similar auxin influx peak positions to the wild type, while the peak values occurred at 0.25 mm from the apex in *phot1 phot2* and *nph3* mutants. In *phot1 phot2* and *nph3* mutants, the peak value was shifted from the position at 0.20 to 0.25 mm from the apex, when the measurements were applied under BL illumination.

We further conducted a two-way analysis of variance (ANOVA) based on the mean peak values ($n = 12$) of the root auxin flux rate to analyze the different BL sensitivities in wild-type and mutant lines (Table 1). The results showed that peak auxin flux values were maintained at a similar basal level in darkness in the wild type and *phot1*, *phot1 phot2*, and *nph3-1* lines, whereas the *pin2* mutants showed a statistically significant difference from wild-type roots in darkness. Furthermore, BL illumination induced a significant difference in the peak auxin flux rate at a position 0.20 mm from the apex, with a strong increase ($>58.9 \text{ fmol}\cdot\text{cm}^{-2}\cdot\text{s}^{-1}$) (Table 1). The peak value of auxin flux rates in seedlings of the

pin2 mutant line was also sensitive to BL, but with a smaller increase in the auxin flux rate of $22.3 \text{ fmol}\cdot\text{cm}^{-2}\cdot\text{s}^{-1}$ (Table 1). However, BL illumination induced no marked increases in auxin flux rates in the root apices of *nph3*, *phot1*, or *phot1 phot2* mutant roots, indicating that phot1 and NPH3 are essential for BL signaling pathways.

To further confirm the effects of BL on auxin distribution in the roots, we analyzed expression of *DR5_{pro}:GFP*, a highly active auxin reporter gene (Ulmasov et al., 1997). Unilateral BL illumination ($2 \mu\text{mol}\cdot\text{m}^{-2}\cdot\text{s}^{-1}$) on the *DR5_{pro}:GFP* root tip resulted in an increase in GFP expression on the shaded side (Figures 2E and 2F). Increasing GFP expression was found up to around 0.3 mm from the root apex in the epidermal and vascular cells after 60 min of unilateral BL illumination (arrowheads in Figure 2F). This result qualitatively supports our discovery of BL-induced auxin influx rate with the noninvasive microelectrode system, which showed that the peak of the auxin influx rate in the root apex was sensitive to BL signals.

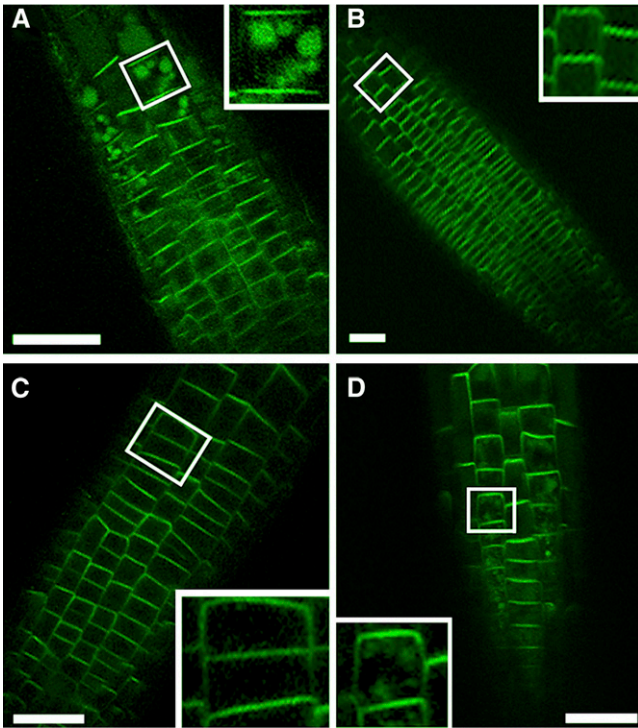


Figure 4. PIN2-GFP Localization and Relocalization in Root Cells under Light and Dark Conditions.

(A) to (D) Images were selected from three independent repeated experiments and at least three seedlings each time. Bars = 20 μm .

(A) Localization of PIN2-GFP in root of a 4-d-old dark-grown seedling; inset shows a detail of PIN2-GFP-positive VLCs.

(B) Localization of PIN2-GFP in root of a 4-d-old light-grown seedling; vacuole-like structures are absent; inset shows details.

(C) Localization of PIN2-GFP in root of a 4-d-old dark-grown seedling, placed in light for the last 12 h; inset shows details.

(D) Localization of PIN2-GFP in root of a 4-d-old light-grown seedling, placed in darkness for the last 12 h; inset shows details of PIN2-GFP-positive VLCs.

[See online article for color version of this figure.]

Brefeldin A and 1-*N*-Naphthylphthalamic Acid Inhibit BL-induced Root Negative Phototropism in *Arabidopsis*

To study the involvement of endosomal membrane recycling in the *Arabidopsis* root apex and to investigate the role of polar auxin transport in phototropic responses, we analyzed the effects of different concentrations of brefeldin A (BFA; an inhibitor of protein secretion and endosomal recycling) (Nebenführ et al., 2002) on BL-induced root phototropism and the root elongation rate. These results showed that BFA treatment at a concentration of more than 20 μM inhibited BL-induced root phototropism completely during the first 9 h of unilateral illumination with 2 $\mu\text{mol}\cdot\text{m}^{-2}\cdot\text{s}^{-1}$ BL (Figure 3A). If the illumination time was prolonged to 24 h, a slight phototropic curvature in the roots still occurred, even at concentrations of 50 μM BFA, which was not stable for such a long period under BL illumination at room temperature. We also measured root growth rates after 5 h BL illumination to statistically analyze root phototropism (Figure 3B)

and the root elongation rate (Figure 3C). As shown in Figure 3B, treatment with 20 μM BFA for 5 h completely prevented root phototropic responses, while only a partial inhibition of root elongation was observed at concentrations below 40 μM . Concentrations of 40 and 50 μM BFA prevented root growth dramatically within 5 h of incubation (Figure 3C). However, deetiolation was not affected, since the cotyledons turned from bright yellow to green (see Supplemental Figure 2 online). To confirm the role of polar auxin transport in root phototropism, we further analyzed the effect of 1-*N*-naphthylphthalamic acid (NPA), an inhibitor of polar auxin transport (Nagashima et al., 2008), on BL-induced root phototropism. As expected, BL-induced root phototropism was inhibited when seedlings were grown on the half-strength Murashige and Skoog (MS) medium containing 0.5 μM NPA (Figure 3D).

BL-Induced Cellular Relocalization of PIN2 Is Dependent on NPH3 and phot1

As previously reported (Kleine-Vehn et al., 2008; Laxmi et al., 2008), in dark-grown roots, PIN2-GFP was largely reduced from the PM, showing less polar localization, and PIN2-GFP-positive vacuole-like compartments (VLCs) were scored in epidermal and cortical cells (Figure 4A). In light-grown roots, PIN2-GFP was polar localized at the PM and within small endosomal vesicles inside the cytosol (Figure 4B). These light- and dark-associated states of PIN2-GFP localization were reversible: Dark incubation caused the reappearance of PIN2-GFP within the VLCs (Figure 4C), and BL irradiation caused the disappearance of VLC-related PIN2-GFP (Figure 4D).

Because the altered BL-induced root gravitropism and phototropism in the *pin2* mutant was complemented by PIN2-GFP protein expression (see Supplemental Figure 3 online; Shin et al., 2005), analyzing these different populations of cellular PIN2 and their roles in root phototropism is reasonable. In the *PIN2_{pro}:PIN2-GFP*-transformed *pin2* mutant seedlings, the disappearance of PIN2-GFP from VLCs was relatively fast under BL irradiation of 2 $\mu\text{mol}\cdot\text{m}^{-2}\cdot\text{s}^{-1}$ (Figure 5A), which was sufficient to initiate a negative phototropic bending in root tips in 30 min (see Supplemental Figure 4 online). In the majority of root cells, PIN2-GFP disappeared from the VLCs after 20 min of irradiation in the *pin2* background (Figure 5A), and the existence of wild-type PIN2 (Col-0 background) did not affect the BL-stimulated behavior of PIN2-GFP (see Supplemental Figure 5 online). In seedlings of the *nph3-1*, *phot1 phot2*, and *phot1* mutant lines expressing PIN2-GFP, the PIN2-GFP was also localized within the VLCs and persisted within VLCs after a 30-min BL illumination (Figures 5B to 5D). However, overnight exposure to BL (12 h) resulted in the disappearance of PIN2-positive VLCs in all these lines (Figure 5), implying that the *phot1/NPH3*-initiated pathway mediates a rapid reaction for the disappearance of PIN2-GFP from VLCs, while prolonged light illumination may switch on other signaling pathways.

phot1 and NPH3 Control BL-Mediated and BFA-Sensitive PIN2 Recycling

Because PIN2 endosomal recycling is essential for polar auxin transport toward the root base (Blilou et al., 2005; Kleine-Vehn

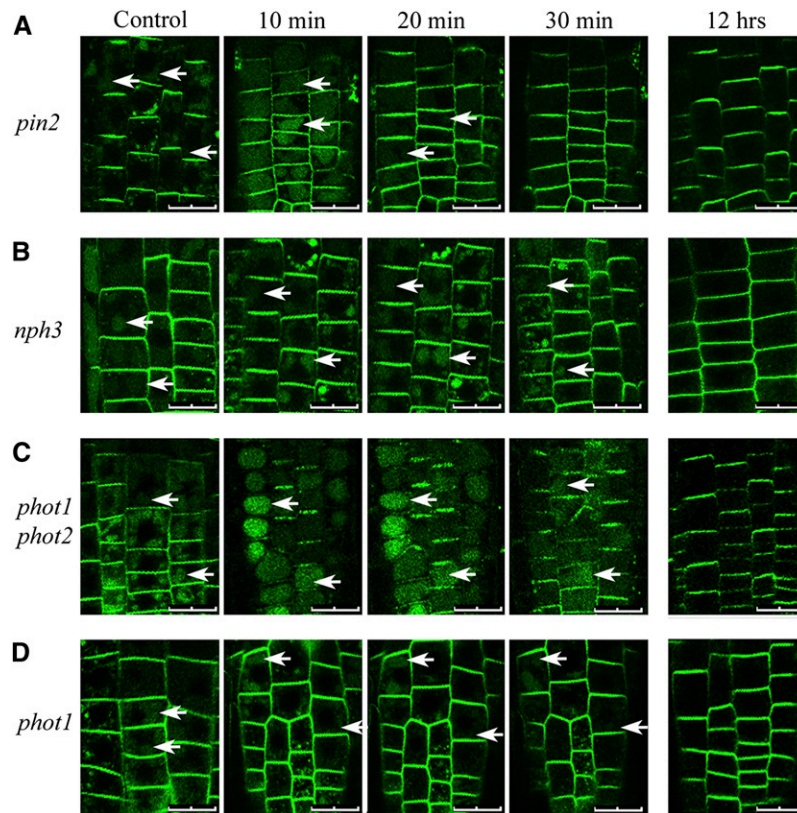


Figure 5. Disappearance of PIN2-GFP from the VLCs Is Dependent on phot1/NPH3.

Arabidopsis seedlings with PIN2-GFP expression on different mutant backgrounds were illuminated with $2 \mu\text{mol}\cdot\text{m}^{-2}\cdot\text{s}^{-1}$ BL for 0, 10, 20, or 30 min or placed under BL overnight (12 h) (columns from left to right). White arrows indicate VLCs. Images were selected from three independent repeated experiments and at least three seedlings each time. Bars = $20 \mu\text{m}$.

(A) BL-induced PIN2-GFP relocalization in a *pin2* background.

(B) BL-induced PIN2-GFP relocalization in an *nph3* background.

(C) BL-induced PIN2-GFP relocalization in a *phot1 phot2* background.

(D) BL-induced PIN2-GFP relocalization in a *phot1* background.

[See online article for color version of this figure.]

and Friml, 2008), the above results suggest that both the lack of PIN2 protein and inhibition of vesicular recycling by BFA-inhibited negative phototropism in *Arabidopsis* roots. Therefore, we further investigated the effects of BFA on PIN2 localization in root cells. Given that $30 \mu\text{M}$ BFA completely prevented BL-induced root phototropism and only partially reduced the root growth rate with 5 h of treatment (Figure 3), we applied $30 \mu\text{M}$ BFA in this study. As shown in Figure 6, treating etiolated PIN2-GFP-transformed *pin2* mutant seedlings with BFA under dark (Figure 6A) and light (Figure 6B) conditions for 60 min caused relocalization of PIN2-GFP into BFA compartments. When dark-grown roots were exposed to BFA in the dark, PIN2-GFP still remained within the VLCs (white arrows in Figure 6A) and became partially localized within the BFA-induced FM4-64-positive compartments (yellow arrows in Figure 6A). By contrast, BFA treatment conducted under BL resulted in more abundant and larger PIN2-GFP-positive BFA compartments with FM4-64 colocalization (yellow arrows in Figure 6B), while PIN2-GFP

disappeared from the VLCs (Figure 6B). The structures of VLCs and BFA-induced compartments are clearly distinguishable in these images. To avoid a potential effect of FM4-64, the marker of PM and endosomes, on membrane trafficking (Jelínková et al., 2010), we repeated this experiment without FM4-64 labeling in different *PIN2_{pro}:PIN2-GFP*-transformed mutant lines. As shown in Figures 6C and 6D, the BFA-induced compartments can be detected in all lines observed, with or without BL illumination. Importantly, the BFA treatment in the *nph3-1* mutant background resulted in the disappearance of PIN2-GFP from VLCs under both dark and light conditions. By contrast, PIN2-GFP was retained within VLCs in *phot1* and *phot1 phot2* mutants under both dark and light conditions. Furthermore, BFA induced enlarged endosomal compartments in all mutant backgrounds examined (Figures 6C and 6D), and the presence of wild-type PIN2 (Col-0 background) did not change the behavior of PIN2-GFP under BFA treatments (see Supplemental Figure 5 online).

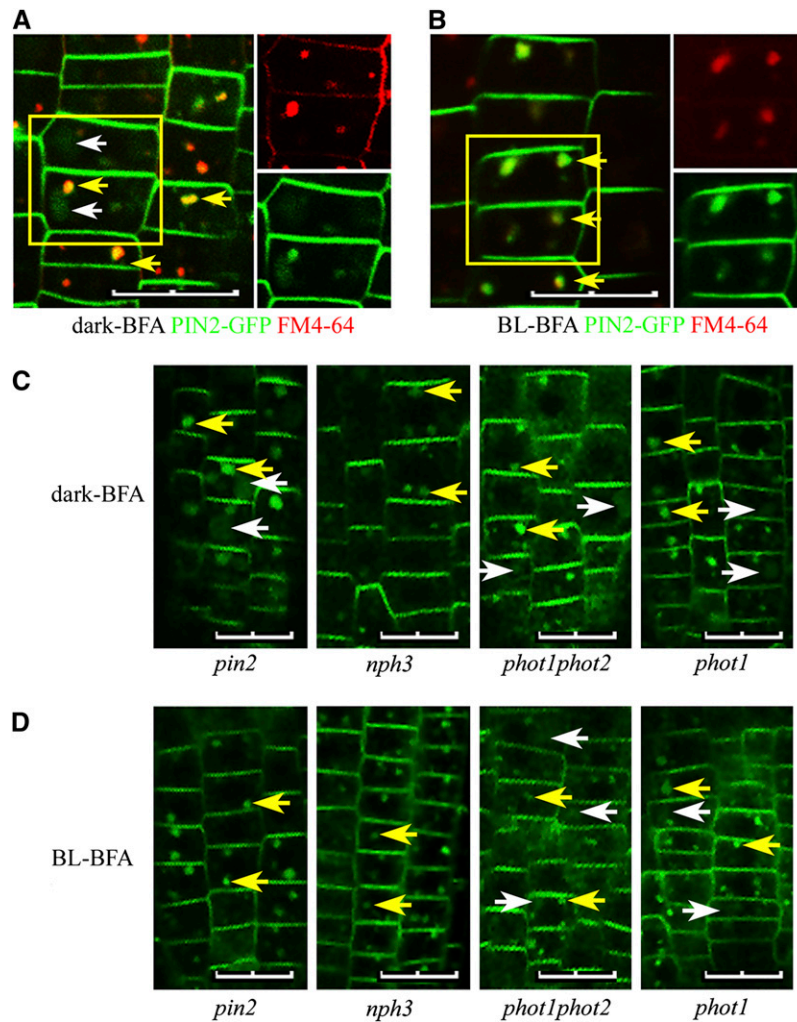


Figure 6. BFA-Sensitive Recycling of PIN2 Is Dependent on BL Illumination.

(A) to (D) Images were selected from three independent repeated experiments and at least three seedlings at each time. Yellow arrows point to BFA-induced compartments; white arrows point to VLCs. Bars = 20 μm .

(A) Four-day-old dark-grown PIN2-GFP transformed seedlings treated with 30 μM BFA and 5 μM FM4-64 under dark conditions for 60 min. Red signals are from FM4-64. PIN2-GFP remained in VLCs without colocalization with the FM4-64 (white arrows); these compartments are smaller, with higher fluorescence densities, than the VLC compartments (yellow arrows), which are not colocalized with FM4-64 (red fluorescence).

(B) Four-day-old dark-grown PIN2-GFP transformed seedlings treated with 30 μM BFA and 5 μM FM4-64 under 2 $\mu\text{mol}\cdot\text{m}^{-2}\cdot\text{s}^{-1}$ BL illumination for 60 min. BL caused the disappearance of PIN2-GFP-positive VLCs and colocalization of both fluorescence signals inside the same BFA compartment.

(C) Images represent *Arabidopsis* seedlings treated with 30 μM BFA for 60 min showing PIN2-GFP expression in different mutant backgrounds under dark conditions. Left to right: *pin2*, *nph3*, *phot1 phot2*, and *phot1*.

(D) Images represent *Arabidopsis* seedlings treated with 30 μM BFA for 60 min showing PIN2-GFP expression in different mutant backgrounds under 2 $\mu\text{mol}\cdot\text{m}^{-2}\cdot\text{s}^{-1}$ BL illumination. Left to right: *pin2*, *nph3*, *phot1 phot2*, and *phot1*.

Gravitropic Bending of Roots in the *phot1*, *phot1 phot2*, and *nph3* Mutant Lines

Because the PIN2 vacuole localization may play roles in gravitropic bending responses (Kleine-Vehn et al., 2008), we investigated whether the absence of *phot1*, *phot2*, both *phot1* and *phot2*, or *NPH3* affected the gravitropic responses of roots under BL illumination. Figure 7 shows the curvature responses in dark-grown seedlings under a 90° gravity stimulation vector for 10 h

following three kinds of light treatment: top-oriented strong white light (10,000 lux) during the gravitropic stimulation to mimic a normal environment, complete darkness during gravity stimulation, and a neutral BL illumination field created by identical and symmetrical weak BL from the front and back of Petri dishes to observe the gravitropic bending response by BL illumination without phototropic signals (Figure 7). Statistical analysis showed no significant difference in the mean values of curvature among the roots of wild-type (*Col-0* and *Ws*), *phot1*, *phot1 phot2*,

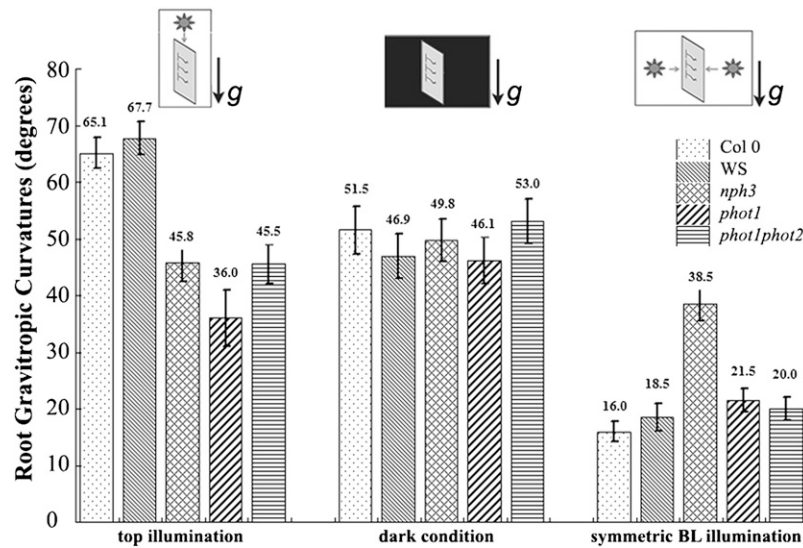


Figure 7. Root Gravitropic Curvature of the Wild Type and *nph3*, *phot1*, and *phot1 phot2* Mutant Lines under Different Light Conditions.

The 4-d-old dark-grown seedlings were turned to a horizontal position (90°), and the root curvature angles were measured and analyzed after 10 h (means \pm SE, $n = 24$). Columns on the left indicate gravitropic curvature with strong white light illumination from above in a culture chamber (10,000 lux); middle columns are gravitropic curvatures in complete darkness; columns on the right indicate gravitropic curvatures in a neutral BL illumination field, created by identical and symmetrical weak BL ($2 \mu\text{mol}\cdot\text{m}^{-2}\cdot\text{s}^{-1}$) from the front and back side of Petri dishes (model figures indicate the illumination method).

and *nph3* mutant lines (Table 2) when compared with the gravity-stimulated bending response in darkness. Using a top-oriented light source during the gravity stimulation, the curvature response in wild-type roots was significantly greater than that in *phot1*, *phot1 phot2*, and *nph3* roots. Compared with the phototropic responses under dark conditions, symmetrical lateral BL illumination gave rise to a dramatic decrease in the bending curvatures in roots of wild-type, *phot1*, *phot1 phot2*, and *nph3* seedlings, among which the *nph3* line showed a minimal effect.

DISCUSSION

Although a gravitropic role for PIN2 in roots was reported over a decade ago (Chen et al., 1998; Luschnig et al., 1998), its role in root phototropic responses has remained unclear. We found that in the absence of PIN2 expression, roots showed a strongly altered ability to grow and bend away from the source of BL illumination, whereas hypocotyl phototropism was barely affected (Figure 1; see Supplemental Figure 1 online). This different behavior was not unexpected, as PIN2 is not expressed in *Arabidopsis* hypocotyls (Chen et al., 1998). Moreover, *in vivo* measurements of auxin flow in the root tips showed that the root apex transition zone (0.1 to 0.3 mm from the root tip in *Arabidopsis*; Verbelen et al., 2006; Baluška et al., 2010) is the most active region with respect to polar auxin flow (Mancuso et al., 2005; Baluška et al., 2010; McLamore et al., 2010; McLamore and Porterfield, 2011) and gravity-stimulated peak cell elongation rates (Chavarria-Krauser et al., 2008). A BL illumination significantly increased the peak value of the auxin flux rate in the root apex transition zone of both dark-grown wild-

type and *pin2* seedlings, among which the response of the *pin2* mutant was less significant than that of the wild type. This result implied that some other auxin transporters might be involved in BL-induced auxin transport besides PIN2. The ABC subfamily B auxin transporter could be a potential candidate because the *pgp19* mutant has a significantly increased root phototropic bending response after 13 h of unilateral BL illumination (see Supplemental Figure 6 online), coincident with early reports on hypocotyl phototropism (Noh et al., 2003; Christie et al., 2011). Considering that the unilateral BL illumination increased asymmetric GFP expression in *DR5_{pro}:GFP* transformed wild-type lines in the root apex transition zone, we conclude that unilateral BL stimulates asymmetric auxin distribution between the shaded and illuminated side by asymmetrically increasing the upward (shootward) polar auxin transport. This conclusion is further supported by the experimental results that NPA, an effective inhibitor of the polar auxin transport, prevented BL-induced negative root phototropism in *Arabidopsis*.

The BL-induced root negative phototropism in *Arabidopsis* is mediated by the BL photoreceptor *phot1* and the signal transducer NPH3 (see Supplemental Figure 7 online). Previous studies also quantified the BL-induced root phototropic bending curvatures in *phot1*, *phot2*, and *nph3* mutants, indicating that *phot2* had a strongly reduced phototropic bending, while *phot1* and *nph3* had almost no bending response (Liscum and Briggs, 1995, 1996; Motchoulski and Liscum, 1999). In agreement with these earlier experiments, we found that the unilateral BL-induced root growth angles separated from the vertical in *phot1* and *phot1 phot2* mutants were similar to each other. Also, a significant difference was observed in the mean values of the auxin flux rate under BL illumination between *phot1* and *phot1 phot2*, while the

Table 2. Two-Way ANOVA for the Gravitropic Curvatures

Comparison Test	Mean Difference	Significant
Significance of differences between lines in top illumination		
TOP: wild type (Col-0) versus wild type (Ws)	2.6	ns
TOP: wild type (Ws) versus <i>nph3</i>	-21.9	**
TOP: wild type (Col-0) versus <i>phot1</i>	-29.1	**
TOP: wild type (Col-0) versus <i>phot1 phot2</i>	-19.6	**
TOP: <i>phot1</i> versus <i>phot1 phot2</i>	9.5	*
TOP: <i>phot1</i> versus <i>nph3</i>	-9.8	*
TOP: <i>nph3</i> versus <i>phot1 phot2</i>	-0.3	ns
Significance of differences between lines in dark condition		
Dark: wild type (Col-0) versus wild-type (Ws)	-4.6	ns
Dark: wild type (Ws) versus <i>nph3</i>	2.9	ns
Dark: wild type (Col-0) versus <i>phot1</i>	5.4	ns
Dark: wild type (Col-0) versus <i>phot1phot2</i>	1.5	ns
Dark: <i>phot1</i> versus <i>phot1 phot2</i>	6.9	ns
Dark: <i>phot1</i> versus <i>nph3</i>	3.7	ns
Dark: <i>nph3</i> versus <i>phot1 phot2</i>	3.2	ns
Significance of differences between lines in symmetric BL illumination		
BL: wild type (Col-0) versus wild type (Ws)	2.5	ns
BL: wild type (Ws) versus <i>nph3</i>	20.0	**
BL: wild type (Col-0) versus <i>phot1</i>	5.5	ns
BL: wild type (Col-0) versus <i>phot1 phot2</i>	4.0	ns
BL: <i>phot1</i> versus <i>phot1phot2</i>	-1.5	ns
BL: <i>phot1</i> versus <i>nph3</i>	-17.0	**
BL: <i>nph3</i> versus <i>phot1 phot2</i>	-18.5	**
Significance of differences between different light conditions		
Wild type (Col-0): TOP versus dark	-13.6	*
Wild type (Col-0): TOP versus BL	-49.1	**
Wild type (Col-0): BL versus dark	35.5	**
<i>nph3</i> : TOP versus dark	4.0	ns
<i>nph3</i> : TOP versus BL	-7.3	ns
<i>nph3</i> : BL versus dark	11.3	*
<i>phot1</i> : TOP versus dark	10.1	*
<i>phot1</i> : TOP versus BL	-14.5	*
<i>phot1</i> : BL versus dark	24.6	**
<i>phot1 phot2</i> : TOP versus dark	7.5	ns
<i>phot1 phot2</i> : TOP versus BL	-25.5	**
<i>phot1 phot2</i> : BL versus dark	33.0	**

Two-way ANOVAs were performed to compare significant differences between mean values of gravitropic bending curvatures of the wild-type and mutant lines under different illumination. The illumination methods and mutant lines were set as the two sources of variation, and both caused extremely significant differences ($P < 0.001$). The Bonferroni correction was then applied for comparisons among pairs. The results of comparisons are between the wild type and mutant lines under top-oriented illumination (TOP), between the wild type and mutant lines under dark conditions (dark), between the wild type and mutant lines under asymmetric BL illumination, and between measurements under different illumination methods in each line. ns, no significance; *, $P < 0.05$; **, $P < 0.001$.

peak value in *phot1 phot2* was similar to that of the *nph3* line. This result indicated that the scaffold protein NPH3 modifies auxin transport in *Arabidopsis* roots by transducing the BL signal from *phot1* and *phot2* BL receptors. Pedmale and Liscum (2007) reported that NPH3 is in a phosphorylated state under dark conditions and that BL illumination causes NPH3 dephosphorylation via a *phot1*-dependent mechanism. Note that exposure to auxin stimulated NPH3 in the phosphorylated state, but the phosphorylation state of *phot1* was not affected by auxin treatment (Chen et al., 2010). Obviously, NPH3 has a direct role in the auxin feedback response, whereas *phot1* is not relevant in this respect.

The phenomenon that GFP-tagged proteins accumulate in VLCs in darkness and then disappear following BL illumination is

not a novel finding (Tamura et al., 2003). An earlier report suggested that PIN2 proteolysis is involved in the polar auxin transport and gravitropic bending responses in *Arabidopsis* roots (Abas et al., 2006). Kleine-Vehn et al. (2008) further reported an asymmetric PIN2 distribution for VLCs between the upper and lower sides of gravistimulated roots, implying a close relationship between vacuole-targeted trafficking of PIN2 and gravitropic bending responses. Laxmi et al. (2008) observed that different PIN2-GFP localized in various mutant backgrounds between dark- and light-grown seedlings; however, the short-term reaction of PIN2-GFP under BL illumination was not documented. In agreement with an earlier study reporting that BL-induced phototropism is a rapid response (Steinitz and Poff, 1986), we found that a short BL illumination can stimulate a negative phototropic

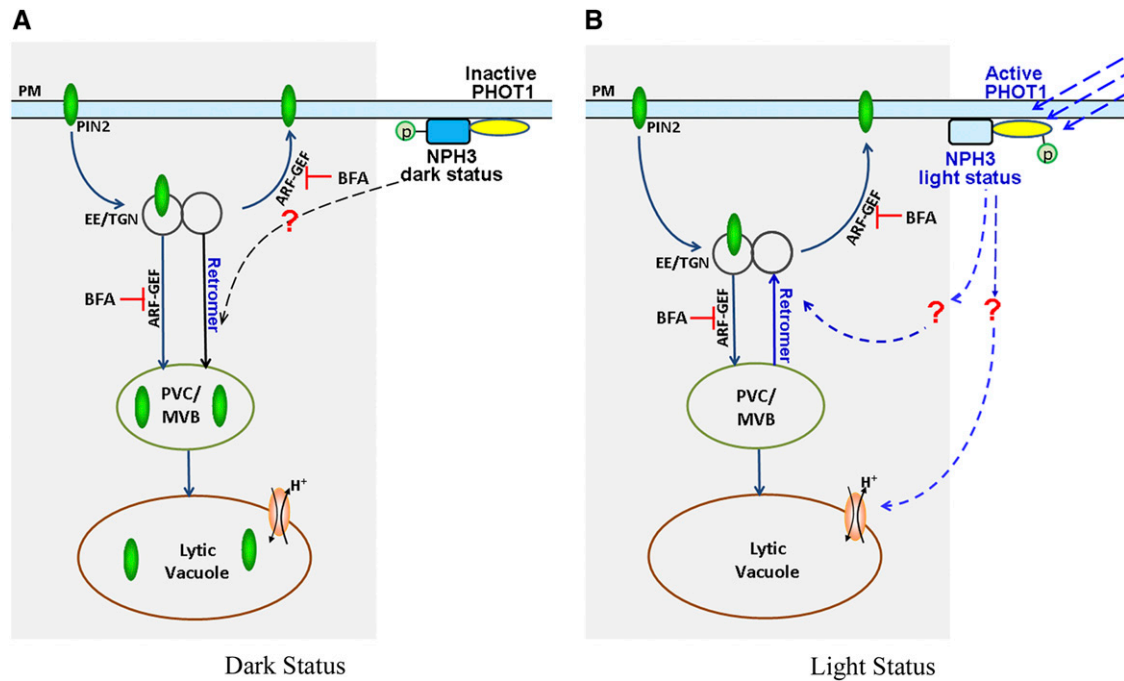


Figure 8. Hypothetical Model Representing the Roles of *phot1* and NPH3 in Endosomal Targeting of PIN2 Proteins.

Shaded areas are based on the early hypothesis (Kleine Vehn et al., 2008), while bright areas are based on our results to explain PIN2 localization and dynamics in darkness and under BL illumination. Membrane-localized *phot1* acts as a BL photoreceptor to activate the signal transducer scaffold protein NPH3 (Wan et al., 2008; Roberts et al., 2011). NPH3 plays role in switching the dynamic equilibrium of PIN2 between PVC-targeting trafficking and membrane-targeting recycling. Furthermore, PIN2 degradation could be controlled through an NPH3-mediated process. ARF, ADP-ribosylation factor; EE, early endosome; GEF, guanine-nucleotide exchange factor; MVB, multivesicular body; PVC, prevacuolar compartment; TGN, *trans*-Golgi network.

bending response in roots (see Supplemental Figure 4 online) and cause complete disappearance of PIN2-GFP from VLCs in the wild-type and *pin2* root cells. Also, a lack of *phot1*/NPH3 expression prevented the disappearance of PIN2-GFP from VLCs after short BL illumination (30 min). However, prolonged BL illumination (12 h) caused the disappearance of VLC-localized PIN2-GFP in *phot1*, *phot1 phot2*, and *nph3* mutants. Therefore, we conclude that the *phot1*/NPH3-mediated PIN2 disappearance from VLCs in root cells is a rapid response to modify BL-induced negative phototropism, while other long-term responses affect PIN2 localization through *phot1*/NPH3-independent pathways.

With regard to the possible mechanism underlying the VLC-localized GFPs, Kleine-Vehn et al. (2008) proposed a model showing that the retromer-mediated pathway plays essential roles in PIN2 trafficking between VLCs and endosomes through a BFA-sensitive, GNOM-dependent trafficking pathway. In addition, BFA treatment caused accumulation of both PIN2-GFP and *phot1*-GFP within enlarged endosomal compartments (Kleine-Vehn et al., 2008; Kaiserli et al., 2009; Sullivan et al., 2010), suggesting that both PIN2 and *phot1* recycle in a GNOM-dependent manner. We found that PIN2-GFP exhibited different BFA-induced relocalization behaviors between the *nph3* and *phot1* mutant lines, implying that *phot1* and NPH3 play different roles in guiding the endosomal recycling and subcellular targeting of auxin transport (PIN2). Based on these results, we hypothesize that NPH3 acts as a switch to determine trafficking in

the retromer-mediated pathway between PVCs/MVBs and EEs/TGNs. Our update of the model proposed by Kleine-Vehn et al. (2008) is summarized in Figure 8. In the *nph3* mutant, in which the NPH3-based retromer pathway is absent, BFA treatment inhibited the ADP-ribosylation factor–guanine-nucleotide exchange factor–mediated trafficking pathway, which stopped the VLC-targeted trafficking and caused PIN2-GFP to disappear from VLCs, even under the dark BFA treatment. In root cells expressing NPH3, but not *phot1*, the NPH3 remained in the dark state and PIN2 continued to move into VLCs. As a result, dark BFA conditions do not cause the disappearance of PIN2-GFP in *phot1* mutants. A similar relationship between PINs and *phot1*/NPH3 was indeed reported for PID/NPY1 and *phot1*/NPH3, which may act in a similar way to control the polar distribution and cellular behavior of PIN-formed proteins (Cheng et al., 2007; Furutani et al., 2007, 2011).

Because *phot1* and NPH3 play roles in controlling the auxin flux rate in the root apical transition zone, we were curious to understand the roles of *phot1* and NPH3 in the integration of gravitropic and phototropic responses in the root tip region. In *Arabidopsis* hypocotyls, the photoreceptor phytochrome A mediates BL-induced inhibition of gravitropism (Lariguet and Fankhauser, 2004). Galen et al. (2004, 2007) demonstrated that *phot1* is important for root penetration into the soil, which increased the drought tolerance of *Arabidopsis* seedlings. Our results show that all lines have similar gravitropic bending

curvatures in darkness. Not unexpectedly, top-oriented light increased a downward-bending curvature in the wild type, which was more significant than that in the mutants. Symmetric lateral BL illumination significantly inhibited gravitropism in all lines. Moreover, gravitropic bending curvatures in *nph3* are significantly larger than in the wild-type, *phot1*, and *phot1 phot2* lines, indicating BL illumination inhibits the root gravitropic responses via a *phot1*-independent pathway in which NPH3 may have a role. For example, auxin treatment can influence the phosphorylation state of NPH3 (Chen et al., 2010), implying NPH3 may be involved in an auxin feedback mechanism to cause a bending response under different environmental stimuli. Furthermore, Matsuda et al. (2011) found that *NPH3*-like and *PGP*-like genes have similar expression patterns in the BL perception organ of maize (*Zea mays*) coleoptiles, implying a potential cross-link between different signaling pathways via NPH3/NPY1 scaffold proteins. Although we are uncertain about which photoreceptor (s) is/are involved in this process, no doubt exists that NPH3 not only mediates BL-induced negative root phototropism, but also plays important roles in interactions between gravitropic and phototropic signaling pathways, perhaps by controlling proteasome activities and determining the subcellular destiny of PIN2 in cells of the root apex transition zone.

METHODS

Plant Material

Seeds of *Arabidopsis thaliana* were sterilized in 3% NaClO solution with 0.01% Triton X-100 for 5 min, then washed with sterile water five times. The surface-sterilized seeds were planted on agar plates containing half-strength MS culture medium (Sigma-Aldrich) and 1% Suc (w/v). Plates were cold-treated at 4°C for 24 h before placing in the cultivation chamber at 22°C and 16 h white light illumination (10,000 lux) per day provided by fluorescence lamps for light-grown seedlings. Etiolated seedlings were kept in Petri dishes covered with aluminum foil following the initiation of germination by 2 h of white light illumination at 22°C. The *pin2* mutant line (*eir 1-4*, Col 0 background), *PIN2_{pro}:PIN2-GFP* (*eir 1-1* background), and *DR5_{pro}:GFP* transformed lines were obtained from Rujin Chen (Noble Foundation, Ardmore, OK; Ulmasov et al., 1997; Laxmi et al., 2008). The *nph3-1* mutant line (Ws background) was obtained from Emmanuel Liscum (University of Missouri, Columbia, MO; Motchoulski and Liscum, 1999). The *phot1-5* and *phot1-5/phot2-1* (Col-0 background) mutants and *PHOT1_{pro}:PHOT1-GFP* (*phot1-5* background) transformed lines were obtained from Winslow Briggs (Carnegie Institution for Science, Stanford, CA; Sakamoto and Briggs, 2002). *Pgp19* mutants were obtained from Rongchen Lin (Institute of Botany, Chinese Academy of Sciences; Lin and Wang, 2005). Pollen from the *PIN2_{pro}:PIN2-GFP* (#) transformed plants was crossed onto the mature stigma of *nph3-1*, *phot1-5*, and *phot1 phot2* mutants (§). F1 plants were self-pollinated and grown to the F2 generation. F2 seeds were cultured on the agar surface with lateral light illumination, and seedlings without phototropism were chosen and grown on soil to obtain the F3 generation. Phototropism analysis of F3 lines was performed to identify the homozygous mutant lines with PIN2-GFP expression, which were used for the experiments as indicated above (see Supplemental Figure 3 online). To examine whether the existence of wild-type PIN2 proteins in these lines affected the cellular behavior of PIN2-GFP, we also crossed the *PIN2_{pro}:PIN2-GFP* transformed line (#) onto the wild type (Col-0, §) to obtain heterozygous plants. The F1 plants were used as a control (see Supplemental Figure 5 online).

Phototropic Growth Analysis

Seeds were sterilized, planted as described above, and put on the same plates in two parallel lines with one line of Col-0 seeds. An LED was used to create parallel side illumination at $2 \mu\text{mol m}^{-2} \text{s}^{-1}$. Therefore, the seedlings were side-illuminated from the beginning of their germination, and the lean angles of both roots were recorded by a digital camera after 4 d (96 h). Separation angles between the position of the root or shoot tips and the vertical position instead of root tip bending angles were manually measured by the software ImageJ (National Institutes of Health). The relative distribution rate is shown as columns in Figures 1G and 1H. Gaussian fitting curves were calculated out with software Origin 8.0 with the single peak fitting options (with equation: $y = y_0 + (A/(w * \text{sqrt}(\text{PI}/2))) * \exp(-2 * ((x - xc)/w)^2)$).

Phototropic and Gravitropic Bending Analysis

For measuring phototropic bending curvatures, 3-d-old dark-grown seedlings were unilaterally illuminated with $2 \mu\text{mol m}^{-2} \text{s}^{-1}$ BL from a light-emitting diode (LED) in the germination plates. To analyze BFA and NPA effects on phototropism, BFA and NPA were diluted into the culture medium at appropriate concentrations. Images were recorded with a digital camera at specific time points. For analysis of gravitropism, 3-d-old etiolated seedlings were turned 90°. Images were recorded with a digital camera after 10 h, and the mean values and standard errors of the separation or bending angles were calculated.

Measurement of Auxin Flow in the Root Apex Region

The measurement of rhizosphere auxin flux in this noninvasive microelectrode system was based on the application of Fick's law [$J = -D(\Delta C/\Delta X)$] (J , flux rate of analytes; ΔC , concentration differences; ΔX , distance between two positions; D , diffusion coefficient, $D_{\text{auxin}} = 0.677 \times 10^{-5} \text{ cm}^2 \text{ s}^{-1}$ at 25°C) (Mancuso et al., 2005; McLamore et al., 2010). Measurement of the rhizosphere auxin flux reflex activity of cell-to-cell auxin transport, which occurs in the apoplast, provides a quantitative analysis of polar auxin transport (McLamore et al., 2010; McLamore and Porterfield, 2011). A carbon nanotube auxin-selective microelectrode was used to monitor auxin fluxes in *Arabidopsis* roots as described previously (Mancuso et al., 2005; Santelia et al., 2005; Bouchard et al., 2006; Bailly et al., 2008; Kim et al., 2010). For measurements, plants were grown in hydroponic culture and used at 4 d after germination. Microelectrodes were set near the root surface at different distances from the root apex, vibrating typically between 2 and 12 μm from the surface ($\Delta X = 10 \mu\text{m}$). Then, the auxin flux rate was recorded in the absence or presence of BL. The latter condition was obtained with a blue LED (peak wavelength 473 nm); the seedlings were only exposed to BL during measurement. No preillumination was performed in this study.

Statistical Analysis

Statistical differences of data in Figures 2 and 7 were analyzed with two-way ANOVA (Tables 1 and 2). The paired Student's t test was applied to test significance between measured groups with only one variance (Figure 3; see Supplemental Figures 1, 2, and 6 online). Two-tailed P values were recorded. Statistical significances were clarified as no significance: * $P < 0.05$; ** $P < 0.001$.

Confocal Laser Scanning Microscopy and Image Processing

The images were obtained with a Leica TCS SP5 laser scanning confocal microscope system. A $\times 10$ air objective (numerical aperture [NA] = 0.4), $\times 40$ air objective (NA = 0.75), and a $\times 63$ water immersion objective (NA = 1.2) were used. An argon laser provided BL (488 nm). Emission fluorescence was

obtained for GFP signals (500 to 530 nm) and FM4-64 (600 to 700 nm) with band-pass filters. To create a pseudo-color image that visualizes the signal intensities of GFP (Figures 2E and 2F), the original images were obtained from the same confocal microscope with same laser and camera settings and then the images were transferred to index color format using ImageJ software (National Institutes of Health) with the Rainbow-LUT spectral setting. All parameters were kept constant for image processing.

Chemical and BL Treatment

BFA (Sigma-Aldrich; 5 mg/mL) and NPA (Sigma-Aldrich; 5 mg/mL) were stored as DMSO solutions in a -20°C freezer, and FM4-64 [*N*-(3-triethylammoniumpropyl)-4-(6-(4-(diethylamino)phenyl)hexatrienyl)pyridinium dibromide; purchased from Sigma-Aldrich as Synaptored; 1 mg/mL] was stored as a water solution at 4°C in the refrigerator and kept in dark condition. Half-strength MS basal salts and 1% Suc in water were used as solvents for inhibitor working solutions: BFA and NPA with appropriate concentrations and $5\ \mu\text{M}$ FM4-64. The seedlings were treated with various working solution in Eppendorf tubes in darkness within individual period described in figure legends. All operations were done under a weak green light provided by LEDs in a dark room. If experiments required continuous BL illumination, seedlings were transferred onto a glass slide for exposure in a drop of the inhibitor solution. A different and adjustable BL source for continuous BL illumination was provided by a LED light source with a peak wavelength at 473 nm. The BL was measured with a Sanwa power meter (model Sanwa LP1). All the experiments were conducted in a dark room equipped with a weak, green LED light.

Accession Numbers

Sequence data from this article can be found in the Arabidopsis Genome Initiative or GenBank/EMBL databases under the following accession numbers: AT3G45780, AT5G58140, AT5G64330, and AT5G57090.

Supplemental Data

The following materials are available in the online version of this article.

Supplemental Figure 1. BL-Induced Phototropic Curvature in the *pin2* Mutant Line.

Supplemental Figure 2. BL-Induced Phototropic Responses of *Arabidopsis* on BFA-Containing Agar Plates.

Supplemental Figure 3. BL-Induced Phototropic Responses in the *PIN2-GFP*-Expressed *Arabidopsis* Lines.

Supplemental Figure 4. BL-Induced Phototropic Response of a Dark-Grown Wild-Type *Arabidopsis* Root.

Supplemental Figure 5. The Wild-Type PIN2 Does Not Affect the BL-Induced and BFA-Induced Behavior of PIN2-GFP.

Supplemental Figure 6. BL-Induced Phototropic Response of Dark-Grown Wild-Type and *pgp19* *Arabidopsis* Root.

Supplemental Figure 7. BL-Induced Phototropic Response in Dark-Grown Wild-Type, *phot1 phot2*, *phot1*, and *nph3* *Arabidopsis* Seedlings.

Supplemental Table 1. Mean Values of Auxin Influx Flow in *Arabidopsis* Root Apex.

ACKNOWLEDGMENTS

We thank Winslow Briggs (Carnegie Institution for Science) for patient editing of the manuscript and for providing the *phot1*, *phot1phot2* mutant lines and the *PHOT1_{PRO}:PHOT1-GFP* transformed line. We

thank Zhenqing Li (Institute of Botany, Chinese Academy of Sciences) for guiding the statistic analysis in the manuscript, Haiyang Wang (Beijing Kaituo Research Center) and Youfa Cheng (Institute of Botany, Chinese Academy of Sciences) for critical reading of the manuscript, and Rongcheng Lin (Institute of Botany, Chinese Academy of Sciences) for providing the *pgp19* mutant line. We also thank Emmanuel Liscum (University of Missouri) for providing *nph3-1* mutant seeds and Rujin Chen (Noble Foundation) for providing seeds of the *PIN2_{PRO}:PIN2-GFP* and *DR5_{PRO}:GFP* transgenic *Arabidopsis* lines. Y.W. thanks Halina Gabryś (University of Kraków) for introducing him to the research field of photobiology. Y.W. and J.L. are supported by the National Basic Research Program of China (973 Program 2011CB809103 and 2011CB944601), the Chinese Academy of Sciences/State Administration of Foreign Expert Affairs International Partnership Program for Creative Research Teams (20090491019), the National Natural Science Foundation of China (31000595, 30730009 and 30821007), the Knowledge Innovation Program of the Chinese Academy of Sciences (KJJCX2-YW-L08 and KSCX2-EW-J-1) and the China Postdoctoral Science Foundation. F.B. receives partial support from the Grant Agency Vedecká Grantová Agentúra (Bratislava, Slovakia; Project 2/0200/10) and from the Grant Agency Agentúra na Podporu Výskumu a Vývoja (Bratislava, Slovakia; Project APVV-0432-06). Grants from Bundesministerium für Wirtschaft und Technologie via Deutsches Zentrum für Luft- und Raumfahrt (Cologne, Germany; Project 50WB 0434), the European Space Agency-European Space Research and Technology Centre (Noordwijk, The Netherlands; MAP Project AO-99-098), and the Ente Cassa di Risparmio di Firenze (Italy) are gratefully acknowledged.

AUTHOR CONTRIBUTIONS

Y.W., F.B., and J.L. designed this project. Y.W. performed the research, analyzed the data, and wrote the article. J.J. crossed the *Arabidopsis* lines. L.W. and H.H. performed analysis on phototropism and gravitropism. S.M. supported the noninvasive measurement of auxin flux. D.V., D.M., F.B., and J.L. revised and edited this article. F.B. and J.L. contributed equally in supervising this project.

Received November 30, 2011; revised February 4, 2012; accepted February 13, 2012; published February 28, 2012.

REFERENCES

- Abas, L., Benjamins, R., Malenica, N., Paciorek, T., Wisniewska, J., Moulinier-Anzola, J.C., Sieberer, T., Friml, J., and Luschnig, C. (2006). Intracellular trafficking and proteolysis of the *Arabidopsis* auxin-efflux facilitator PIN2 are involved in root gravitropism. *Nat. Cell Biol.* **8**: 249–256.
- Bailly, A., Sovero, V., Vincenzetti, V., Santelia, D., Bartnik, D., Koenig, B.W., Mancuso, S., Martinoia, E., and Geisler, M. (2008). Modulation of P-glycoproteins by auxin transport inhibitors is mediated by interaction with immunophilins. *J. Biol. Chem.* **283**: 21817–21826.
- Baluška, F., Mancuso, S., Volkmann, D., and Barlow, P.W. (2010). Root apex transition zone: A signalling-response nexus in the root. *Trends Plant Sci.* **15**: 402–408.
- Blakeslee, J.J., Bandyopadhyay, A., Peer, W.A., Makam, S.N., and Murphy, A.S. (2004). Relocalisation of the PIN1 auxin efflux facilitator plays a role in phototropic responses. *Plant Physiol.* **134**: 28–31.
- Bllou, I., Xu, J., Wildwater, M., Willemsen, V., Paponov, I., Friml, J., Heidstra, R., Aida, M., Palme, K., and Scheres, B. (2005). The PIN

- auxin efflux facilitator network controls growth and patterning in *Arabidopsis* roots. *Nature* **433**: 39–44.
- Boonsirichai, K., Guan, C., Chen, R., and Masson, P.H.** (2002). Root gravitropism: An experimental tool to investigate basic cellular and molecular processes underlying mechanosensing and signal transmission in plants. *Annu. Rev. Plant Biol.* **53**: 421–447.
- Bouchard, R., Bailly, A., Blakeslee, J.J., Oehring, S.C., Vincenzetti, V., Lee, O.R., Paponov, I., Palme, K., Mancuso, S., Murphy, A.S., Schulz, B., and Geisler, M.** (2006). Immunophilin-like TWISTED DWARF1 modules auxin efflux activities of *Arabidopsis* P-glycoproteins. *J. Biol. Chem.* **281**: 30603–30612.
- Chavarría-Krauser, A., Nagel, K.A., Palm, K., Schurr, U., Walter, A., and Scharr, H.** (2008). Spatio-temporal quantification of differential growth processes in root growth zones based on a novel combination of image sequence processing and refined concept describing curvature production. *New Phytol.* **177**: 811–821.
- Chen, R., Hilson, P., Sedbrook, J., Rosen, E., Caspar, T., and Masson, P.H.** (1998). The *Arabidopsis thaliana* AGRAVITROPIC 1 gene encodes a component of the polar-auxin-transport efflux carrier. *Proc. Natl. Acad. Sci. USA* **95**: 15112–15117.
- Chen, Y., Hoehenwarter, W., and Weckwerth, W.** (2010). Comparative analysis of phytohormone-responsive phosphoproteins in *Arabidopsis thaliana* using TiO₂-phosphopeptide enrichment and mass accuracy precursor alignment. *Plant J.* **63**: 1–17.
- Cheng, Y., Qin, G., Dai, X., and Zhao, Y.** (2007). NPY1, a BTB-NPH3-like protein, plays a critical role in auxin-regulated organogenesis in *Arabidopsis*. *Proc. Natl. Acad. Sci. USA* **104**: 18825–18829.
- Christensen, S.K., Dagenais, N., Chory, J., and Weigel, D.** (2000). Regulation of auxin response by the protein kinase PINOID. *Cell* **100**: 469–478.
- Christie, J.M., et al.** (2011). phot1 Inhibition of ABCB19 primes lateral auxin fluxes in the shoot apex required for phototropism. *PLoS Biol.* **9**: e1001076.
- Correll, M.J., and Kiss, J.Z.** (2002). Interactions between gravitropism and phototropism in plants. *J. Plant Growth Regul.* **21**: 89–101.
- Ding, Z.J., Galván-Ampudia, C.S., Dermarsy, E., Łangowski, Ł., Kleine-Vehn, J., Fan, Y.W., Morita, M.T., Tasaka, M., Fankhauser, C., Offringa, R., and Friml, J.** (2011). Light-mediated polarization of the PIN3 auxin transporter for the phototropic response in *Arabidopsis*. *Nat. Cell Biol.* **13**: 447–452.
- Friml, J., et al.** (2004). A PINOID dependent binary switch in apical-basal PIN polar targeting directs auxin efflux. *Science* **306**: 862–865.
- Furutani, M., Kajiwara, T., Kato, T., Tremli, B.S., Stockum, C., Torres-Ruiz, R.A., and Tasaka, M.** (2007). The gene MACCHI-BOU 4/ENHANCER OF PINOID encodes a NPH3-like protein and reveals similarities between organogenesis and phototropism at the molecular level. *Development* **134**: 3849–3859.
- Furutani, M., Sakamoto, N., Yushida, S., Kajiwara, T., Robert, H.S., Friml, J., and Tasaka, M.** (2011). Polar-localised NPH3-like proteins regulate polarity and endocytosis of PIN-FORMED auxin efflux carriers. *Development* **138**: 2069–2078.
- Galen, C., Huddle, J., and Liscum, E.** (2004). An experimental test of the adaptive evolution of phototropins: Blue-light photoreceptors controlling phototropism in *Arabidopsis thaliana*. *Evolution* **58**: 515–523.
- Galen, C., Rabenold, J.J., and Liscum, E.** (2007). Functional ecology of a blue light photoreceptor: effects of phototropin-1 on root growth enhance drought tolerance in *Arabidopsis thaliana*. *New Phytol.* **173**: 91–99.
- Galván-Ampudia, C.S., and Offringa, R.** (2007). Plant evolution: AGC kinases tell the auxin tale. *Trends Plant Sci.* **12**: 541–547.
- Holland, J.J., Roberts, D., and Liscum, E.** (2009). Understanding phototropism: From Darwin to today. *J. Exp. Bot.* **60**: 1969–1978.
- Jelínková, A., Malínská, K., Simon, S., Kleine-Vehn, J., Parezová, M., Pejchar, P., Kubes, M., Martinec, J., Friml, J., Zazimalová, E., and Petrášek, J.** (2010). Probing plant membranes with FM dyes: Tracking, dragging or blocking? *Plant J.* **61**: 883–892.
- Kaiserli, E., Sullivan, S., Jones, M.A., Feeney, K.A., and Christie, J.M.** (2009). Domain swapping to assess the mechanistic basis of *Arabidopsis* phototropin 1 receptor kinase activation and endocytosis by blue light. *Plant Cell* **21**: 3226–3244.
- Kim, J.Y., Henrichs, S., Bailly, A., Vincenzetti, V., Sovero, V., Mancuso, S., Pollmann, S., Kim, D., Geisler, M., and Nam, H.G.** (2010). Identification of an ABCB/P-glycoprotein-specific inhibitor of auxin transport by chemical genomics. *J. Biol. Chem.* **285**: 23309–23317.
- Kleine-Vehn, J., and Friml, J.** (2008). Polar targeting and endocytic recycling in auxin-dependent plant development. *Annu. Rev. Cell Dev. Biol.* **24**: 447–473.
- Kleine-Vehn, J., Leitner, J., Zwiewka, M., Sauer, M., Abas, L., Luschnig, C., and Friml, J.** (2008). Differential degradation of PIN2 auxin efflux carrier by retromer-dependent vacuolar targeting. *Proc. Natl. Acad. Sci. USA* **105**: 17812–17817.
- Lariguet, P., and Fankhauser, C.** (2004). Hypocotyl growth orientation in blue light is determined by phytochrome A inhibition of gravitropism and phototropin promotion of phototropism. *Plant J.* **40**: 826–834.
- Lau, O.S., and Deng, X.W.** (2010). Plant hormone signalling lightens up: Integrators of light and hormones. *Curr. Opin. Plant Biol.* **13**: 1–7.
- Laxmi, A., Pan, J., Morsy, M., and Chen, R.** (2008). Light plays an essential role in intracellular distribution of auxin efflux carrier PIN2 in *Arabidopsis thaliana*. *PLoS ONE* **3**: e1510.
- Li, Y., Dai, X., Cheng, Y., and Zhao, Y.** (2011). NPY genes play an essential role in root gravitropic responses in *Arabidopsis*. *Mol. Plant* **4**: 171–179.
- Lin, R., and Wang, H.** (2005). Two homologous ATP-binding cassette transporter proteins, AtMDR1 and AtPGP1, regulate *Arabidopsis* photomorphogenesis and root development by mediating polar auxin transport. *Plant Physiol.* **138**: 949–964.
- Liscum, E., and Briggs, W.R.** (1995). Mutations in the NPH1 locus of *Arabidopsis* disrupt the perception of phototropic stimuli. *Plant Cell* **7**: 473–485.
- Liscum, E., and Briggs, W.R.** (1996). Mutations of *Arabidopsis* in potential transduction and response components of the phototropic signalling pathway. *Plant Physiol.* **112**: 291–296.
- Luschnig, C., Gaxiola, R.A., Grisafi, P., and Fink, G.R.** (1998). EIR1, a root-specific protein involved in auxin transport, is required for gravitropism in *Arabidopsis thaliana*. *Genes Dev.* **12**: 2175–2187.
- Mancuso, S., Marras, A.M., Magnus, V., and Baluška, F.** (2005). Non-invasive and continuous recordings of auxin fluxes in intact root apex with a carbon-nanotube-modified and self-referencing microelectrode. *Anal. Biochem.* **341**: 344–351.
- Mancuso, S., Marras, A.M., Mugnai, S., Schlicht, M., Zarsky, V., Li, G., Song, L., Xue, H.W., and Baluška, F.** (2007). Phospholipase D ζ 2 drives vesicular secretion of auxin for its polar cell-cell transport in the transition zone of the root apex. *Plant Signal Behav.* **2**: 240–244.
- Matsuda, S., Kajizuka, T., Kadota, A., Nishimura, T., and Koshiba, T.** (2011). NPH3- and PGP-like genes are exclusively expressed in the apical tip region essential for blue-light perception and lateral auxin transport in maize coleoptiles. *J. Exp. Bot.* **62**: 3459–3466.
- McLamore, E.S., Diggs, A., Calvo Marzal, P., Shi, J., Blakeslee, J.J., Peer, W.A., Murphy, A.S., and Porterfield, D.M.** (2010). Non-invasive quantification of endogenous root auxin transport using an integrated flux microsensor technique. *Plant J.* **63**: 1004–1016.
- McLamore, E.S., and Porterfield, D.M.** (2011). Non-invasive tools for measuring metabolism and biophysical analyte transport: Self-referencing physiological sensing. *Chem. Soc. Rev.* **40**: 5308–5320.

- Michniewicz, M., et al.** (2007). Antagonistic regulation of PIN phosphorylation by PP2A and PINOID directs auxin flux. *Cell* **130**: 1044–1056.
- Monshausen, G.B., and Gilroy, S.** (2009). The exploring root–root growth responses to local environmental conditions. *Curr. Opin. Plant Biol.* **15**: 1855–1866.
- Motchoulski, A., and Liscum, E.** (1999). *Arabidopsis* NPH3: A NPH1 photoreceptor interacting protein essential for phototropism. *Science* **286**: 961–964.
- Nagashima, A., Uehara, Y., and Sakai, T.** (2008). The ABC subfamily B auxin transporter AtABC19 is involved in the inhibitory effects of N-1-naphthylphthalamic acid on the phototropic and gravitropic responses of *Arabidopsis* hypocotyls. *Plant Cell Physiol.* **49**: 1250–1255.
- Nebenführ, A., Ritzenthaler, C., and Robinson, D.G.** (2002). Brefeldin A: Deciphering an enigmatic inhibitor of secretion. *Plant Physiol.* **130**: 1102–1108.
- Noh, B., Bandyopadhyay, A., Peer, W.A., Spalding, E.P., and Murphy, A.S.** (2003). Enhanced gravi- and phototropism in plant *mdr* mutants mislocalizing the auxin efflux protein PIN1. *Nature* **423**: 999–1002.
- Pedmale, U.V., and Liscum, E.** (2007). Regulation of phototropic signalling in *Arabidopsis* via phosphorylation state changes in the phototropin 1-interacting protein NPH3. *J. Biol. Chem.* **282**: 19992–20001.
- Rahman, A., Takahashi, M., Shibasaki, K., Wu, S., Inaba, T., Tsurumi, S., and Baskin, T.I.** (2010). Gravitropism of *Arabidopsis thaliana* roots requires the polarization of PIN2 toward the root tip in meristematic cortical cells. *Plant Cell* **22**: 1762–1776.
- Robert, H., and Friml, J.** (2009). Auxin and other signals on the move in plants. *Nat. Chem. Biol.* **5**: 325–332.
- Roberts, D., Pedmale, U. V., Morrow, J., Sachdev, S., Lechner, E., Tang, X., Zheng, N., Hannink, M., Genschik, P., and Liscum E.** (2011). Modulation of phototropic responsiveness in *Arabidopsis* through ubiquitination of phototropin 1 by the CUL3-ring E3 ubiquitin ligase CRL3^{NPH3}. *Plant Cell* **23**: 3627–3640.
- Sakamoto, K., and Briggs, W.R.** (2002). Cellular and subcellular localization of phototropin 1. *Plant Cell* **14**: 1723–1735.
- Santelia, D., Vincenzetti, V., Azzarello, E., Bovet, L., Fukao, Y., Düchtig, P., Mancuso, S., Martinoia, E., and Geisler, M.** (2005). MDR-like ABC transporter AtPGP4 is involved in auxin-mediated lateral root and root hair development. *FEBS Lett.* **579**: 5399–5406.
- Shin, H., Shin, H.S., Guo, Z., Blancaflor, E.B., Masson, P.H., and Chen, R.** (2005). Complex regulation of *Arabidopsis* AGR1/PIN2-mediated root gravitropic response and basipetal auxin transport by cantharidin-sensitive protein phosphatases. *Plant J.* **42**: 188–200.
- Steinitz, B., and Poff, K.L.** (1986). A single positive phototropic response induced with pulsed light in hypocotyls of *Arabidopsis thaliana* seedlings. *Planta* **168**: 305–315.
- Sukumar, P., Edwards, K.S., Rahman, A., Delong, A., and Muday, G.K.** (2009). PINOID kinase regulates root gravitropism through modulation of PIN2-dependent basipetal auxin transport in *Arabidopsis*. *Plant Physiol.* **150**: 722–735.
- Sullivan, S., Kaiserli, E., Tseng, T.S., and Christie, J.M.** (2010). Subcellular localisation and turnover of *Arabidopsis* phototropin1. *Plant Signal. Behav.* **5**: 184–186.
- Takahashi, H., Miyazawa, Y., and Fujii, N.** (2009). Hormonal interactions during root tropic growth: Hydrotropism versus gravitropism. *Plant Mol. Biol.* **69**: 489–502.
- Tamura, K., Shimada, T., Ono, E., Tanaka, Y., Nagatani, A., Higashi, S.I., Watanabe, M., Nishimura, M., and Hara-Nishimura, I.** (2003). Why green fluorescent fusion proteins have not been observed in the vacuoles of higher plants. *Plant J.* **35**: 545–555.
- Ulmasov, T., Murfett, J., Hagen, G., and Guilfoyle, T.J.** (1997). Aux/IAA proteins repress expression of reporter genes containing natural and highly active synthetic auxin response elements. *Plant Cell* **9**: 1963–1971.
- Verbelen, J.P., De Cnodder, T., Le, J., Vissenberg, K., and Baluška, F.** (2006). The root apex of *Arabidopsis thaliana* consist of four distinct zone of growth activities: meristematic zone, transition zone, fast elongation zone and growth terminating zone. *Plant Signal. Behav.* **1**: 296–304.
- Wan, Y.L., Eisinger, W., Ehrhardt, D., Kubitscheck, U., Baluška, F., and Briggs, W.** (2008). The subcellular localisation and blue-light-induced movement of phototropin 1-GFP in etiolated seedlings of *Arabidopsis thaliana*. *Mol. Plant* **1**: 103–117.
- Whippo, C.W., and Hangarter, R.P.** (2006). Phototropism: Bending towards enlightenment. *Plant Cell* **18**: 1110–1119.